


Roman-indigenous interaction in the Salas River valley (Northwest Iberia): the Roman camp of Alto da Raia and its archaeological landscape

INTERACCIÓN ROMANO-INDÍGENA EN EL VALLE DEL RÍO SALAS (NOROESTE PENINSULAR): EL CAMPAMENTO ROMANO DEL ALTO DA RAIA Y SU PAISAJE ARQUEOLÓGICO

João Fonte

Department of Archaeology and History, University of Exeter
j.fonte3@exeter.ac.uk  0000-0003-0367-0598
(Corresponding author)


João Pedro Tereso

CIBIO, Research Center in Biodiversity and Genetic Resources,
InBIO Associate Laboratory, Campus de Vairão, University of Porto
joaotereso@cibio.up.pt  0000-0003-0871-8255


Filipe Costa Vaz

CIBIO, Research Center in Biodiversity and Genetic Resources,
InBIO Associate Laboratory, Campus de Vairão, University of Porto
filipe.mcvaz@gmail.com  0000-0002-9347-3282


Ana Luísa Rodrigues

Centro de Ciências e Tecnologias Nucleares (C²TN),
Departamento de Engenharia e Ciências Nucleares (DECN),
Instituto Superior Técnico, Universidade de Lisboa
alsr@ctn.tecnico.ulisboa.pt  0000-0001-8652-2923


Maria Isabel Dias

Centro de Ciências e Tecnologias Nucleares (C²TN),
Departamento de Engenharia e Ciências Nucleares (DECN),
Instituto Superior Técnico, Universidade de Lisboa
isadias@ctn.tecnico.ulisboa.pt  0000-0002-7033-0502

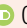
Rosa Marques

Centro de Ciências e Tecnologias Nucleares (C²TN),
Departamento de Engenharia e Ciências Nucleares (DECN),
Instituto Superior Técnico, Universidade de Lisboa
rmarques@ctn.tecnico.ulisboa.pt  0000-0001-6239-5456


Dulce Russo

Centro de Ciências e Tecnologias Nucleares (C²TN),
Departamento de Engenharia e Ciências Nucleares (DECN),
Instituto Superior Técnico, Universidade de Lisboa
dulcef@ctn.tecnico.ulisboa.pt  0000-0003-4954-217X


Patrícia Monteiro

LARC – Laboratório de Arqueociências,
Direção Geral do Património Cultural, ICArHEB,
Interdisciplinary Centre for Archaeology and Evolution of Human
Behaviour,
Universidade do Algarve
patriciamonteiro@dgpc.pt  0000-0002-4606-9201


Mariana Costa Rodrigues

CIBIO, Research Center in Biodiversity and Genetic Resources,
InBIO Associate Laboratory, Campus de Vairão, University of Porto,
marianabccr@cibio.up.pt  0000-0002-6783-1250


Tiago do Pereiro

Era-Arqueologia
tiagopereiro@era-arqueologia.pt  0000-0003-2691-4583


José Carvalho

Era-Arqueologia
josecarvalho@era-arqueologia.pt  0009-0002-2754-2945


Francisco Raimundo

Era-Arqueologia
franciscoraimundo@era-arqueologia.pt  0009-0001-9573-2911


Vanessa Cardoso

Era-Arqueologia
vanessacardoso@era-arqueologia.pt  0009-0003-7017-7186


Carlos Jorge

Era-Arqueologia
carlosjorge@era-arqueologia.pt  0009-0000-2704-6074


Jesús García Sánchez

Instituto de Arqueología Mérida (IAM),
CSIC-Junta de Extremadura
j.garcia@iam.csic.es  0000-0001-7766-1972


Manuel Gago

Departamento de CC. da Comunicación,
Universidade de Santiago de Compostela
manuel.gago.marino@usc.es  0000-0002-5902-6569


José Alberto Gonçalves

Departamento de Geociências,
Ambiente e Ordenamento do Território,
Faculdade de Ciências, Universidade do Porto
jagoncal@fc.up.pt  0000-0001-9212-4649


Emmanuelle Meunier

Casa de Velázquez,
École des Hautes Études Hispaniques et Ibériques (EHEHI)
emmanuelle.meunier@alumni.casadevelazquez.org  0000-0002-1982-9631

Nuno Oliveira

Lab2PT,
Universidade do Minho
ntco_arque@sapo.pt  0000-0002-8720-9469

Ioana Oltean

Department of Archaeology and History,
University of Exeter
i.a.oltean@exeter.ac.uk  0000-0003-2768-525X

Fonte, J., Tereso, J. P., Costa Vaz, F., Rodrigues, A. L., Dias, M. I., Marques, R., Russo, D., Monteiro, P., Costa Rodrigues, M., do Pereiro, T., Carvalho, J., Raimundo, F., Cardoso, V., Jorge, C., García Sánchez, J., Gago, M., Gonçalves, J. A., Meunier, E., Oliveira N. y Oltean, I. (2024): "Roman-indigenous interaction in the Salas River valley (Northwest Iberia): the Roman camp of Alto da Raia and its archaeological landscape", *Spal*, 33.1, pp. 137-163. <https://dx.doi.org/10.12795/spal.2024.i33.06>

Abstract This paper discusses the archaeological research and historical contextualisation of the Alto da Raia enclosure located on the border between northern Portugal and Galicia, identified as a possible Roman camp, following an interdisciplinary and multi-proxy approach. This included archaeological excavation, remote sensing and geophysical survey, as well as sample collection for archaeobotanical and geochemical studies by means of chemical and mineralogical analyses and absolute dating using radiocarbon and luminescence protocols.

The results seem to indicate that this site was a Roman camp probably built and occupied between the 1st century BC and the 1st century AD, when major changes occurred in Northwest Iberia driven by the expansion of the Roman State. The camp overlaps with previous prehistoric occupations possibly dating back to the Bronze Age and Iron Age.

Keywords Roman camp, Remote sensing, Geophysics, Radiocarbon and Luminescence dating, Geochemistry, Archaeobotany.

Resumen Este trabajo aborda la investigación arqueológica y la contextualización histórica del recinto del Alto da Raia, situado en la frontera entre el norte de Portugal y Galicia, identificado como posible campamento romano, siguiendo un enfoque interdisciplinar y multiproxy. Esto incluyó excavación arqueológica, teledetección y prospección geofísica, así como recogida de muestras para estudios arqueobotánicos y geoquímicos mediante análisis químicos y mineralógicos y datación absoluta mediante protocolos de radiocarbono y luminiscencia.

Los resultados parecen indicar que este yacimiento fue un campamento romano y que fue construido y ocupado probablemente entre el siglo I a.C. y el siglo I d.C., cuando se produjeron importantes cambios en el noroeste de Iberia impulsados por la expansión del Estado romano. El campamento se solapa con ocupaciones prehistóricas anteriores que posiblemente se remontan a la Edad del Bronce y a la Edad del Hierro.

Palabras clave Campamento romano, Teledetección, Geofísica, Datación por radiocarbono y luminiscencia, Geoquímica, Arqueobotánica.

1. THE ALTO DA RAIA ENCLOSURE AND ITS ARCHAEOLOGICAL LANDSCAPE

The Alto da Raia enclosure was recently located through remote sensing in the Salas River valley on the border between Portugal (Montalegre) and Galicia (Calvos de Randín). The enclosure has a rectangular layout, with rounded corners and straight lines connecting them, occupying an area of approximately three hectares. It was built on a hill with a maximum altitude of 883 metres, with its rear located at its highest part to the north and sloping slightly downwards to the south towards the Salas River valley which it controls visually. This valley is a natural east-west routeway between the Larouco Mountain and the Lima River, marked since Prehistory by burial mounds (Eguileta Franco, 2003). The enclosure is defined by an earthen embankment, generally quite flattened and almost imperceptible on the southern side. In addition, there is an external ditch, nowadays filled, that complemented its defence. The morphology and location of the site fit very well with a Roman military camp.

The study of the Roman military presence in northern Portugal and southern Galicia has recently undergone significant advances, revealing a great diversity and diachrony of activities and materialities (Costa-García *et al.*, 2019; Fonte *et al.*, 2022; Fonte *et al.*, 2023). Alto da Raia is the first potential Roman military site of temporary nature to be identified in the Salas valley. The nearby permanent fort of *Aquis Querquennis* (Bande, Ourense) in the Lima valley dates to the second half of the 1st century AD, postdating the Roman conquest of Northwest Iberia completed in the late 1st century BC (Rodríguez Colmenero and Ferrer Sierra, 2006; Puente *et al.*, 2018). The Alto da Raia camp very possibly predates this time, which raises interesting questions regarding the early interaction between the local communities and the Roman army. The site overlooks the Salas River valley, exposed to and surrounded by several Iron Age hillforts (fig. 1).

The wider area raises additional information towards such an interpretation. A hoard composed of several pure-silver ingots was identified in a nearby Iron Age hillfort (Lorenzo Fernández, 1970), placed by Armada and García-Vuelta (2015, p. 375) in the Outeiro da Cerca hillfort, probably to be used as hacksilver (Centeno, 2011) (fig. 1). The charcoal associated with

one of the silver ingots was radiocarbon dated to 213-88 cal BC (Armada and García-Vuelta, 2015). These ingots were not made locally and were probably related to the Roman army movements from southern to northern Iberia (Armada and García-Vuelta, 2021). The most significant Iron Age hillfort in the area is probably at Rubiás, located on a prominent hill immediately east of and intervisible with Alto da Raia. Though it is still practically unknown archaeologically, it controls visually a vast expanse of this valley, and its total extent of 10 ha is larger than normal for this region. The internal plan is distributed along several lines of walls which create artificial housing platforms, cut into the steep slope. Several tin and gold mines, probably Roman in date, were located nearby, adding to the bronze and tin metal-lurgic production identified in the Outeiro de Baltar hillfort (fig. 1) (Figueiredo *et al.*, 2022). Finally, the nearby Saceda hillfort (Vázquez Mato, 2021) seems to be part of a wider phenomenon increasingly visible archaeologically, namely the presence of numerous raised granaries (*horrea*) in hillforts in Northwest Iberia dating from the Late Iron Age to the early Roman period. At least in part, this process has been linked to the presence and supply of grain to the Roman army by the indigenous communities (Salido Domínguez, 2020; Seabra *et al.*, 2020).

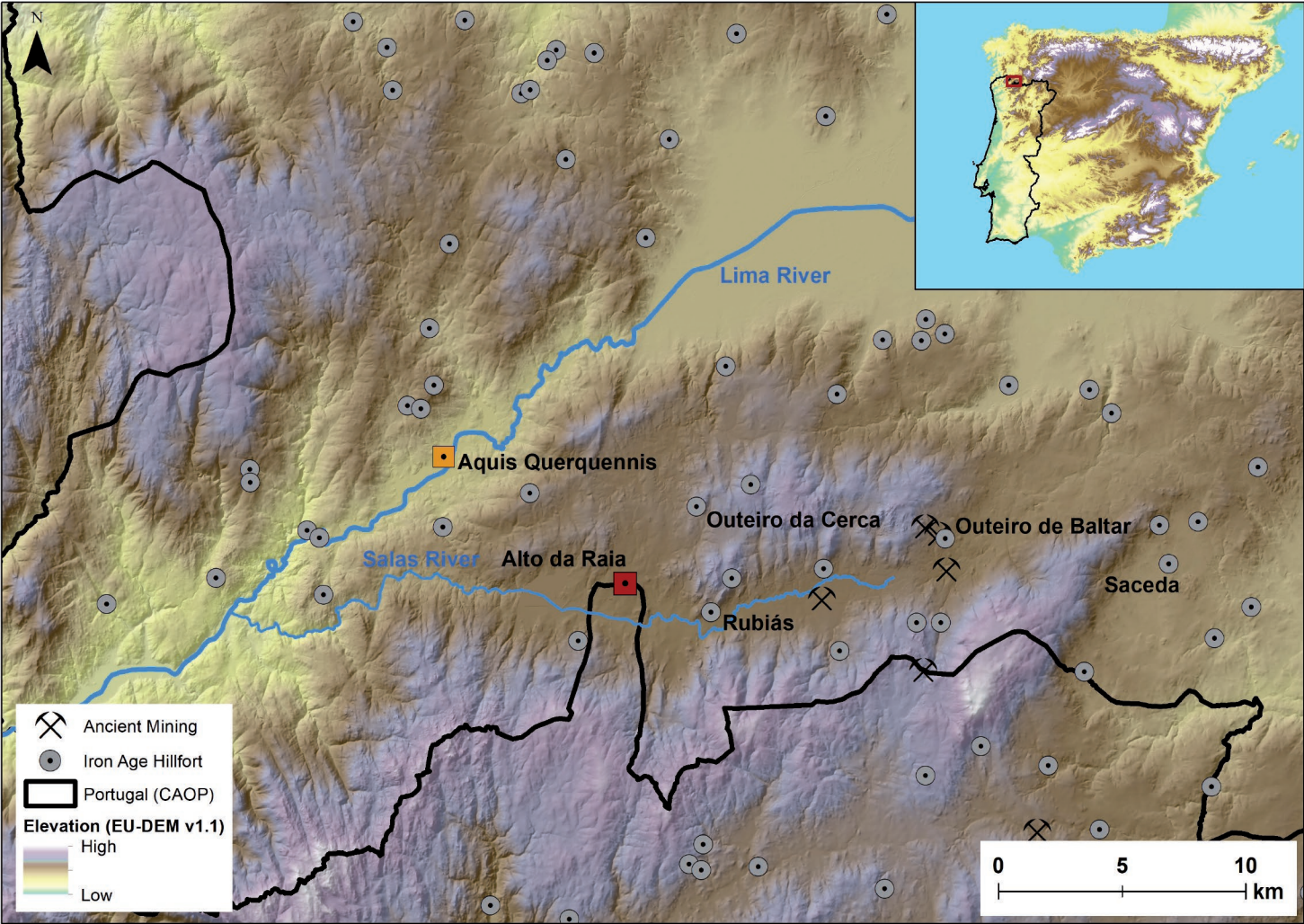


Figure 1. Location of Alto da Raia and its archaeological landscape.

2. MATERIAL AND METHODS

An archaeological survey was recently carried out at Alto da Raia. The main objective was the validation of the site as a Roman military camp and the archaeological investigation and dating of its defensive structure, as well as its historical contextualisation. This survey included remote sensing, geophysical and metal detector survey, archaeological excavation, and sampling for archaeobotanical and geochemical studies and absolute dating.

2.1. Remote Sensing

2.1.1. Airborne LiDAR

The Alto da Raia enclosure was identified from the airborne LiDAR data provided by the Spanish National Geographic Institute (IGN) through the PNOA (*Plan Nacional de Ortofotografía Aérea*) project (<https://pnoa.ign.es/>), which still covers a small part of the Portuguese border. It includes data from two temporal coverages (from 2009 and 2016 for this area), with an average density of 0.5 points per square meter. The point clouds were processed to extract a 1-meter digital terrain model (DTM) from the points automatically classified as ground. From the DTM, different visualization filters were applied to enhance the perception of archaeological features, like local relief model (Hesse, 2010), positive openness (Doneus, 2013), visualization for archaeological topography (VAT) (Kokalj and Somrak, 2019) and sky-view factor (Zakšek et al., 2011) (fig. 2, A). For this, we used a combination of different software, namely LASTools, Relief Visualization Toolbox (RVT) (Kokalj and Somrak, 2019; Zakšek et al., 2011) and planlauf/TERRAIN.

2.1.2. Drone-derived photogrammetric survey

A high-resolution drone photogrammetric survey of the site was completed after vegetation clearance using a DJI Phantom 4 flying at 70 meters above ground level, in order to acquire images with a ground sampling distance (GSD) of 2 cm. A total of 230 images were obtained, covering an area of 360x420 m, with forward and lateral overlaps of 80% and 70% respectively. A set of 10 markers were placed on the ground and surveyed with a GNSS dual frequency receiver, in real-time kinematic (RTK) mode, with a horizontal and vertical accuracy of 2 cm, to act as ground control points (GCP) for accurate georeferencing of the photographs.

The photogrammetric processing was completed using Agisoft Metashape Structure-from-Motion (SfM) and Multi-View-Stereo (MVS) algorithms (Verhoeven, 2011), which first performed an automatic image alignment. Upon identifying the GCPs in the images the dataset becomes rigorously georeferenced, with a total root mean square error (horizontal and vertical) of 3 cm. This allowed for the extraction of geospatial data: a dense point cloud, a digital surface model (DSM) with a grid spacing of 4 cm and an orthomosaic. The DSM was used to produce the orthomosaic. A classification algorithm was then applied to the dense point cloud in Metashape to filter out the ground points from the vegetation (Howland et al., 2022) and generate, based on the former, a highly detailed digital terrain model (DTM) and a hillshade visualization (fig. 2, B). The area was mostly clean of canopied vegetation, so the differences between the DTM and the DSM are minor, but several small trees could be removed from the model, allowing for a better appreciation of the micro-relief of the enclosure.

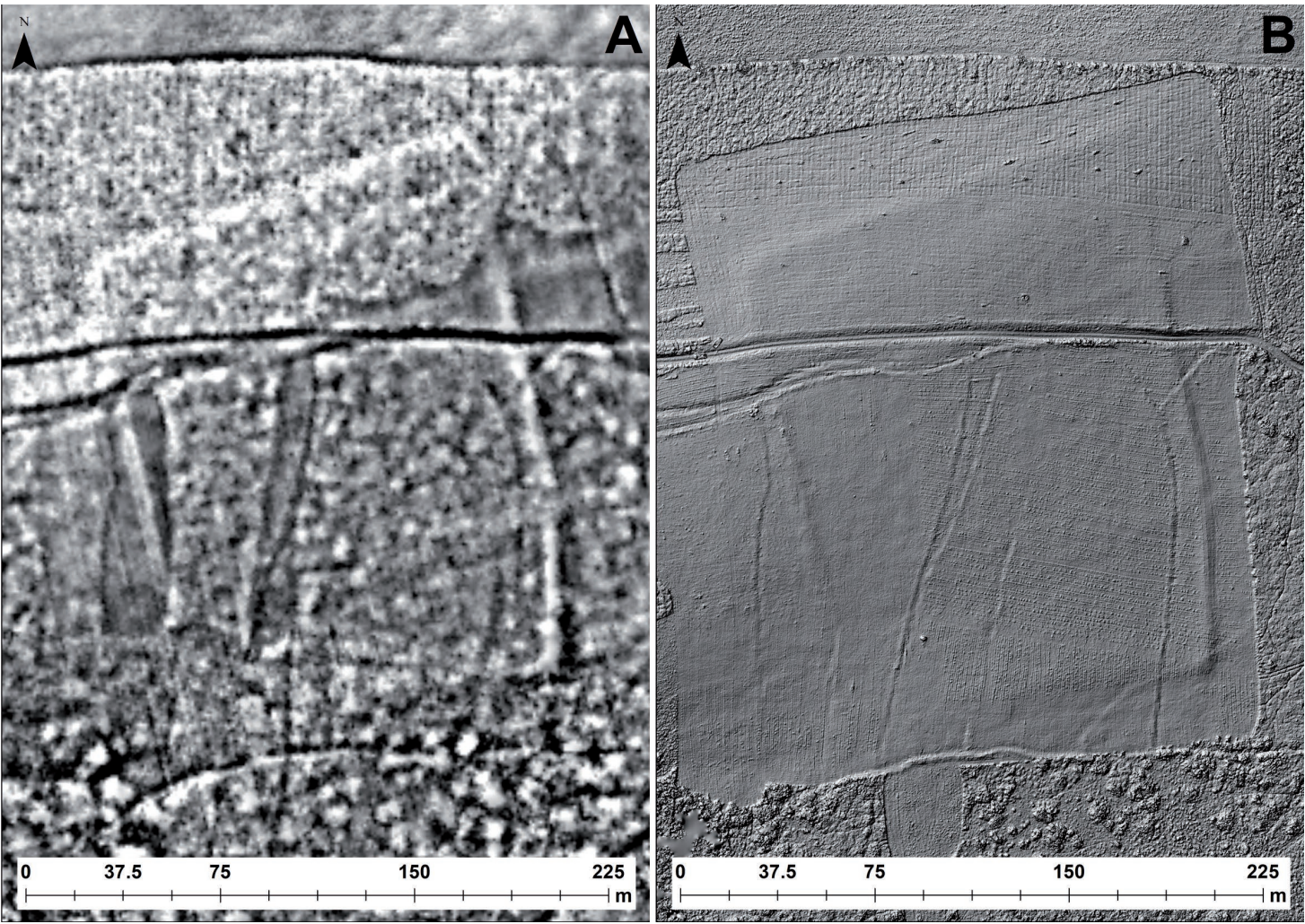


Figure 2. Alto da Raia: IGN-PNOA LiDAR (2009) DTM-derived local relief model (A) and drone DTM-derived hillshade (B).

2.1.3. Geophysics

Both magnetometry and ground-penetrating radar (GPR) surveys were conducted to map the defensive system, in particular the ditch, plus other potential anomalies, like the gates or combustion structures, and to confirm the presence or absence of permanent structures within the enclosure. In addition, and to avoid disturbing archaeological deposits, a metal detector survey was carried out on the modern path that cuts through the site from west to east.

2.1.3.1. Magnetometry survey

The magnetometry survey followed a 30x30 m grid. The first survey covering the entire site was made with a spacing between lines of 1m, and the second, focused on the defensive system, with a tighter spacing between lines of 50 cm (fig. 3, A and B).

It was conducted by using the gradiometer produced by Bartington Instruments – Grad601 with dual Grad-01-1000L sensors mounted on a rigid carrying bar collecting points every 12.5 cm, at a frequency of 50 Hz filter, and automatic collection at 1 m/s. The grid points were georeferenced using an RTK-GNSS Stonex 9A. The collected data were processed in Geoplot 4.0 from Geoscan, using a standard clip between -3nT and +3nT and a Dispike filter applied to remove the intensity of the ferromagnetic peaks. Zero Mean Grid (Threshold = 0.25) and Zero Mean Traverse (Grid=All LMS=On ZM=Mean Thresholds not applied) were also defined to set the background average of each grid and row within each square to zero, eliminating striping effects and discontinuities of lateral limits in the dataset. Two interpolation passes along the line (Interpolate X, Expand - SinX/X, x2) and between paths (Interpolate Y, Expand - SinX/X, x1) were used. The magnetic raster images were georeferenced in QGIS and examined visually for anomalies that might indicate archaeological features, using both different data thresholds or grey scale dynamics as well as intensity, polarization, and geometric shape. This supported interpretation to be drawn in new layers as points, lines and polygons.

141

2.1.3.2. GPR survey

The GPR survey in Alto da Raia was carried out over an area of 15x60 m (900 m²) using equipment and methodology similar to research in other Roman camps in the Iberian northwest (García Sánchez *et al.*, 2022), with the aim to investigate in depth a possible gap on the eastern side of the enclosure (fig. 3). A Noggin 250 Mhz mounted on a Smart-Car by Sensors and Software was used in the survey of Alto da Raia. It was organized in two grids of 15x30 (450 m²) to focus better on the alleged structure. Only the Y transects, perpendicular to the camp's embankment were surveyed with 50 cm between the sensor centre. The Stacking of radar signal was done every 5 cm, and depth of signal recording was set to 90.8 n/s. Radargrams at 10 cm depth slices were processed in Ekko Project, QGIS and visualized in Voxler.

3. RESULTS

This multisensor approach including airborne LiDAR, drone-derived photogrammetry, and magnetic and GPR surveys allowed us to document in a non-invasive way different

realities of the site. The LiDAR and photogrammetry data enabled us to document the embankment and ditch of the camp. The magnetic survey confirmed the full extension of the ditch and more importantly allowed us to identify areas of suspected burning events such as the one excavated in trench 3 (fig. 3, B and C). No permanent built structures were identified. The GPR survey confirmed that the *clavicula* (measures= 5.7 m radius, 10.34 m long inner arch and an outer arch of approximately 14.5 m) accommodated the eastern gate which probably was the case with the three other gates (García-Sánchez *et al.*, 2022) (fig. 3, E). Other features were also detectable at a depth of circa 40 cm below de surface, including a berm separating a ditch from the *clavicula* and the compacted soil that has been interpreted as the bottom of a V-shaped ditch.

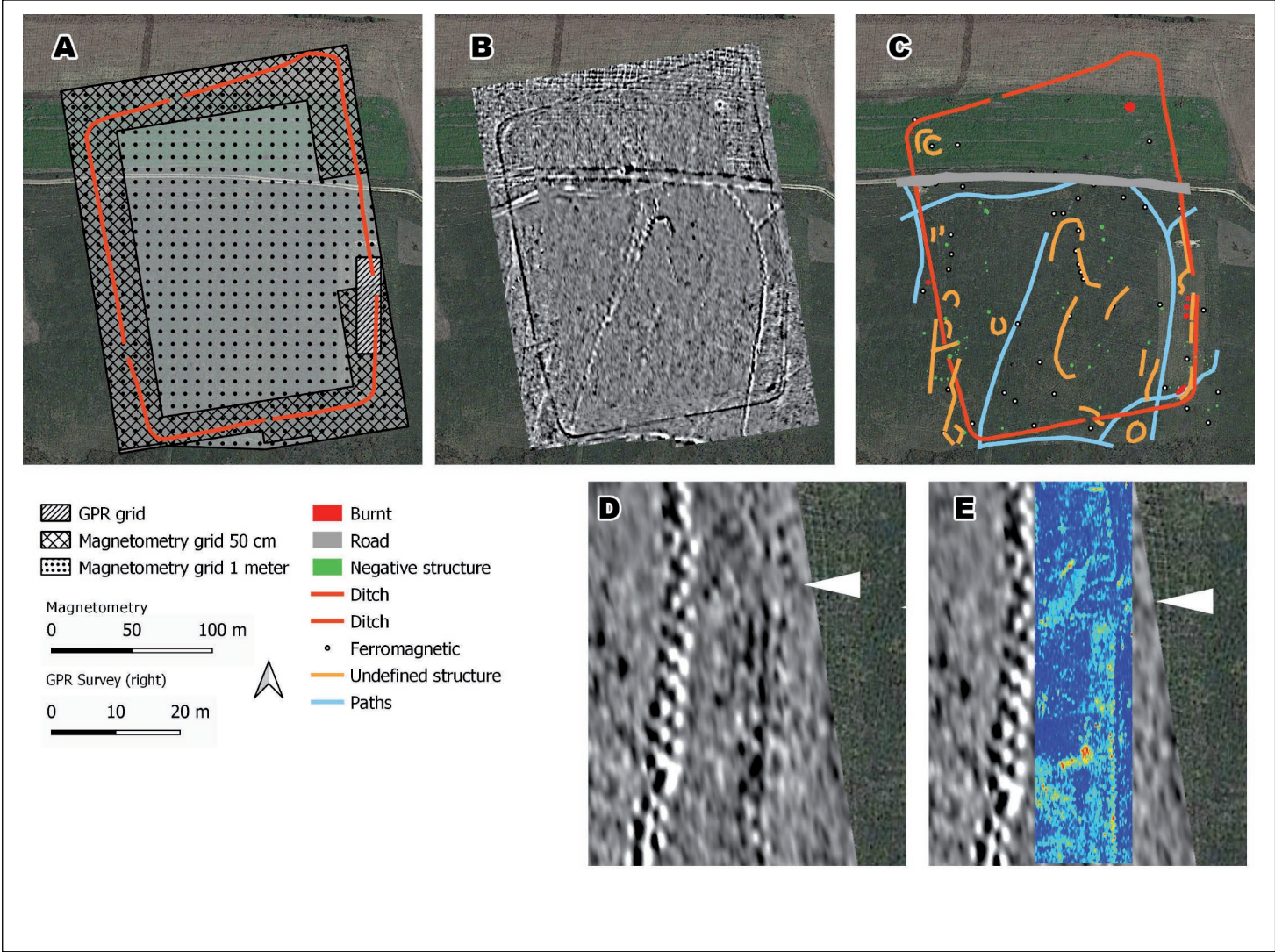


Figure 3. Geophysical coverages on the Alto da Raia enclosure (A); Combination of 50 cm and 1 m magnetometry surveys (B); Interpretation of magnetometry survey (C); Location of the gap on the eastern side of the enclosure, marked with white arrow (D); GPR depth slice at 60-80 cm from the ground level and indication of the location of the *clavicula* (E). Background imagery: Google Satellite.

3.1. Archaeological Excavation

The main objectives of our excavation were the archaeological characterisation and the selection of samples for absolute dating of the Alto da Raia defensive system. Accordingly, two archaeological trenches targeted the defensive system, one on the eastern side (trench 1) and another on the western side (trench 2) (fig. 4). A third trench targeted a magnetic anomaly identified inside the southeastern corner of the enclosure (trench 3) (fig. 4).

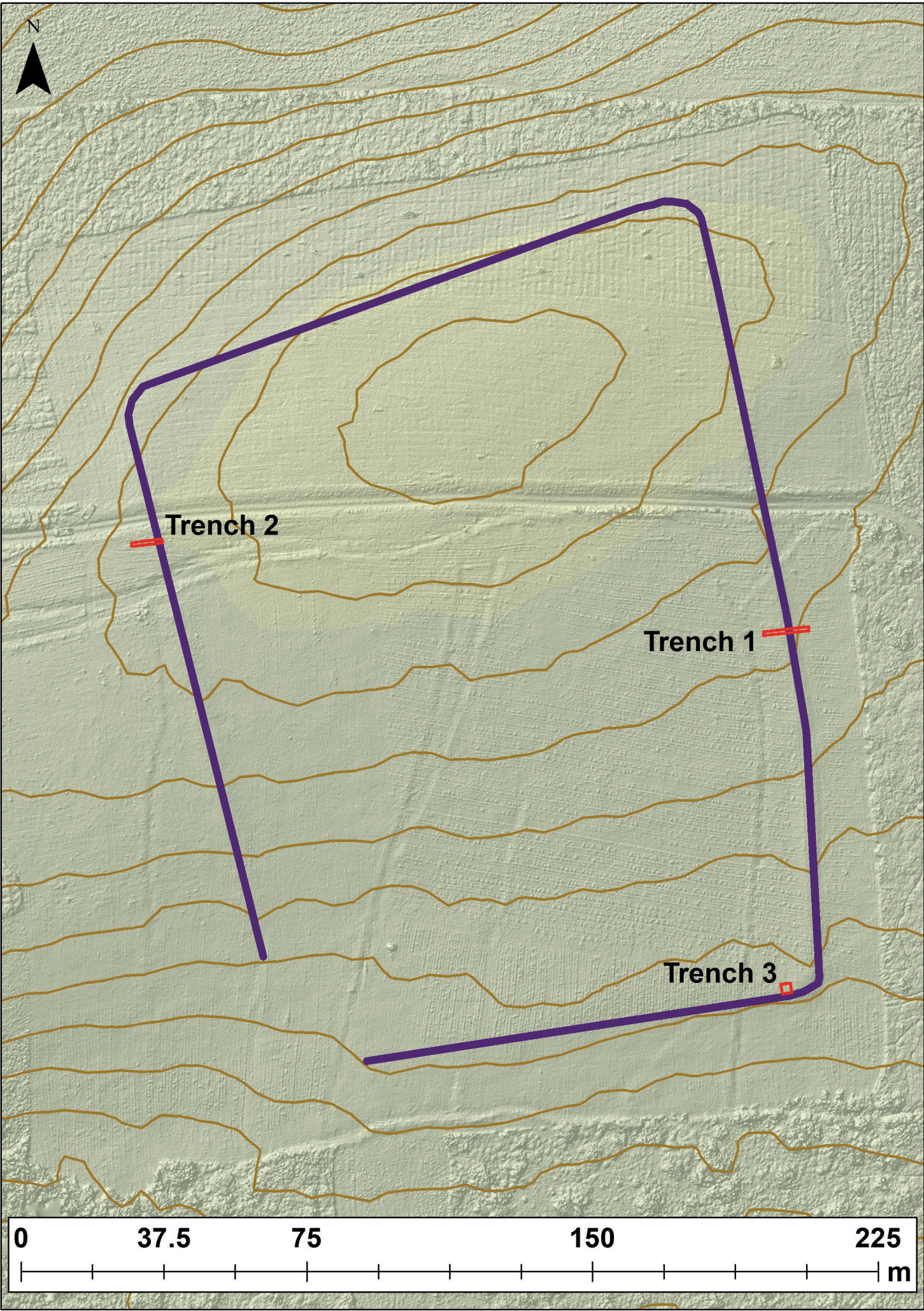


Figure 4. Location of the archaeological trenches in the Alto da Raia enclosure.

3.1.1. Trench 1 (12x1 m)

Trench 1 focused on the eastern part of the Alto da Raia defensive system (figs. 4 and 5) and successfully documented here a V-shaped ditch 2 m wide and 1.5 m deep dug into

the bedrock (SU (Stratigraphic Unit) 110) and with a complex filling consisting of several deposits. The inner embankment built with material taken from the ditch (SU 104) was also documented here. The embankment overlapped an open pit dug into the bedrock (SU 115 and 116) of probable Prehistoric date.

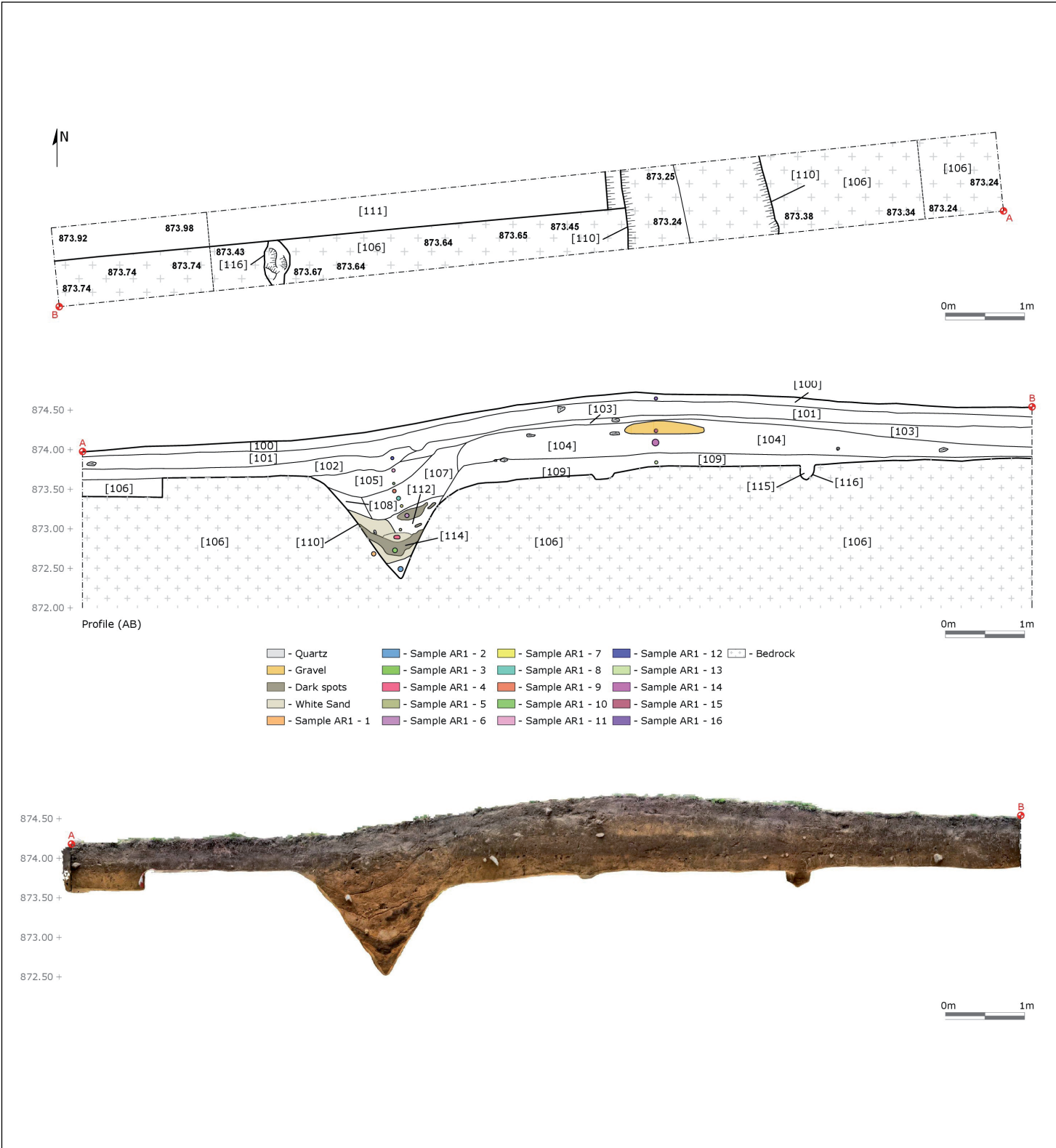


Figure 5. Plan, stratigraphy and samples of trench 1.

3.1.2. Trench 2 (8x1 m)

Trench 2 focused on the western part of its defensive system, again with the aim of archaeologically characterising and dating it (figs. 4 and 6). The same V-shaped ditch of about 2 m in width and 1.5 m in depth dug into the bedrock (SU 208) was documented here, although the filling on this side of the enclosure had a simpler stratigraphy. The inner embankment (SU 206) had been practically levelled due to post-depositional alterations.

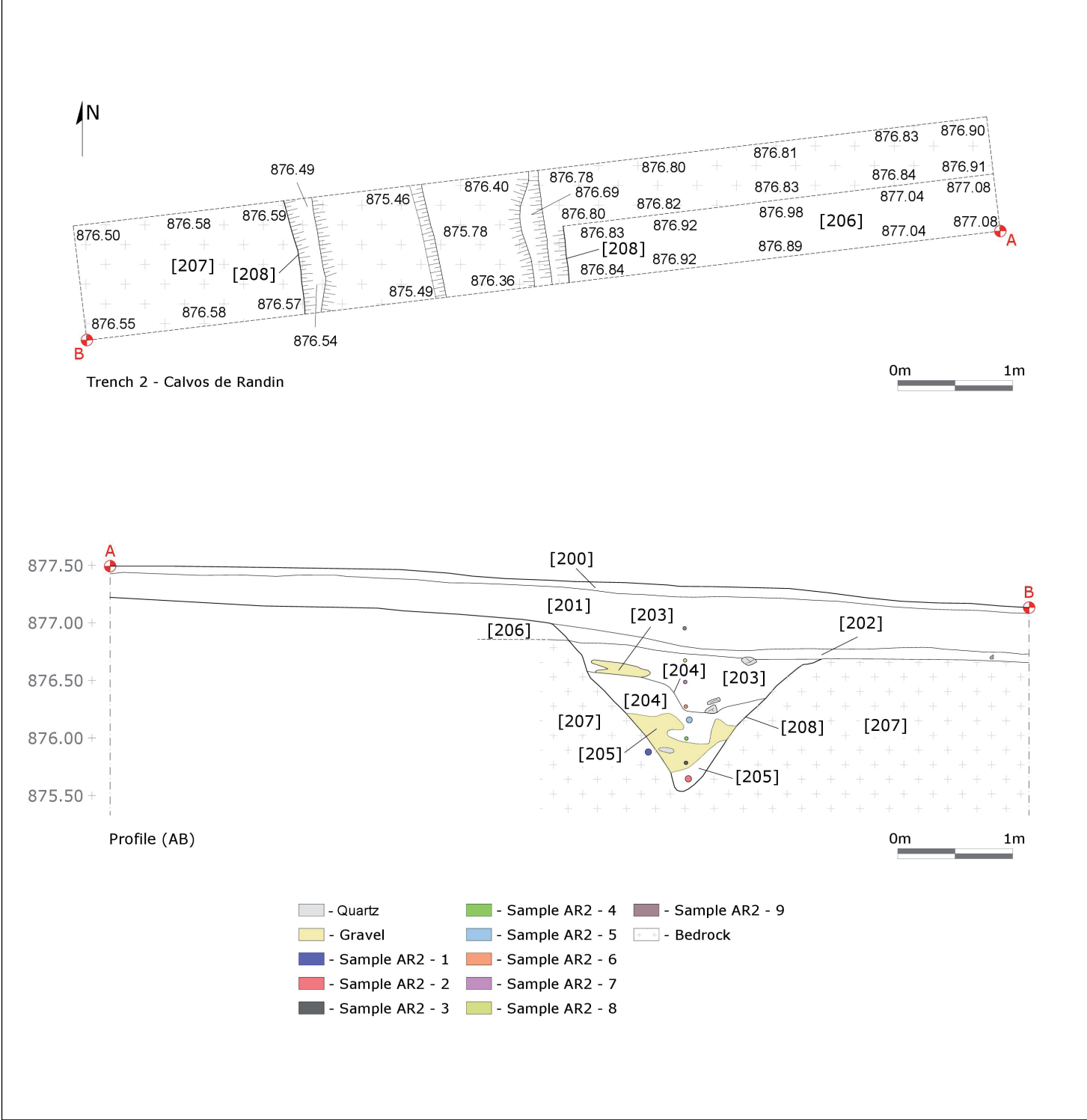


Figure 6. Plan, stratigraphy and samples of trench 2.

3.1.3. Trench 3 (2.5x2.5 m)

Trench 3 focused on an anomaly identified in the magnetic survey (fig. 3), located in the southeast corner of the enclosure (figs. 4 and 7). This turned out to be a double combustion structure excavated on the bedrock with a figure-of-eight shaped in plan (SU 305), consistent in morphology with field ovens found in camps located in other parts of the Roman Empire (e.g., Kenney and Parry, 2012; Arabaolaza, 2019) (fig. 7). Its concave walls and bottom have a reddish colour caused by exposure to high temperatures. Its filling (SU 303 and 307) consisted of charcoal and some charred seeds and fruits. A probable ash pit (SU 306) was documented next to the oven, filled will material (SU 302) taken from the combustion structures. Two notches dug into the bedrock were identified in the walls of the structure (fig. 8). These notches, located between both combustion structures, may be related to the operating system of the oven, serving as a support for its cover, thus retaining heat for longer and slowing down the cooling process.

Figure 7. Plan and stratigraphy of trench 3.



Figure 8. Oven: general view (A) and details of the notches (B and C).

4. SCIENTIFIC LABORATORY ANALYSIS

A sampling strategy for archaeobotanical (anthracology, carpology and dendrology) and geochemical (chemistry and mineralogy) studies and absolute dating (radiocarbon and luminescence) was followed.

4.1. Archaeobotany

Sediment samples were recovered in four SU from Alto da Raia, comprising 43.5 litres of sediment. Most sampling efforts were concentrated in the oven (SU 303 and 307) and ash pit (SU 302) in trench 3, and in one of the filling layers of the ditch (SU 114) in trench 1 where an accumulation of charcoal was identified.

Samples were processed through bucket flotation using meshes of 0.5 mm. Light fractions were sorted to recover fruits and seeds using a stereomicroscope. Wood charcoal fragments of over 2 mm were hand sectioned and the three diagnostic sections were observed under a reflected-light microscope. Identifications of seeds, fruits and wood charcoal were carried out by comparison with material from reference collections and morphological and anatomical atlases (e.g., Schweingruber, 1990; Anderberg, 1994; Vernet *et al.*, 2001; Neef *et al.*, 2012). In order to obtain information regarding the life-history of the tree or shrub, wood-gathering strategies and the fire event that led to its carbonization, each wood fragment was characterized and several dendrological and taphonomical features were recorded such as fragment dimension, tree-ring curvature, evidence of vitrification and radial cracks, among others (Marguerie and Hunot, 2007; McParland *et al.*, 2010; Thery-Parisot and Henry, 2012).

Samples from Alto da Raia were poor in carpological remains (tab. 1). These are particularly rare at the ditch and the SU 302 and are restricted to a few seeds from wild species. In the levels associated with the oven, fruits and seeds are comparatively more frequent. In this structure, rare grains of hulled barley (*Hordeum vulgare*), broomcorn millet (*Panicum miliaceum*) and wheat (*Triticum* sp.) have been found. Unfortunately, the single wheat grain was too damaged to allow a more detailed taxonomic diagnosis. Two glume bases of hulled wheat have also been recovered, most likely belonging to spelt (*Triticum spelta*). A remarkable find is that of a fig seed (*Ficus carica*). The limited abundance and diversity of carpological remains from the oven suggest that the grain was probably introduced as fuel straws to light the fire, ruling out the possibility of a corn dryer (Kenney and Parry, 2012: 255).

The cereals that were found are common in Northwest Iberia both in Late Iron Age and in Early Roman sites. Contrary to other Iberian regions, hulled wheats – mostly spelt – were staple crops in the Late Iron Age and Early Roman sites in Northwest Iberia (Tereso *et al.*, 2013; Teira-Brión, 2019; Peña-Chocarro *et al.*, 2019), probably because they were particularly suited to the mountainous and humid conditions of the area, where they provided higher yields than naked wheats. Their presence at the site may relate to local supply routes, but further studies in this and other Roman camps and Late Iron Age hillforts in the region are necessary to test this hypothesis.

Though fig trees are native to Iberia, it is unlikely that they grew in the wild in the surrounding area of Alto da Raia. Therefore, the presence of a fruit in this context suggests its consumption by the army, as attested elsewhere in the empire (Cavallo *et al.*, 2008), and brought on site from an unknown location. Both fig seeds (Seabra *et al.*, 2023; Tereso *et al.*, 2023) and wood (Figueiral, 1990; Vaz *et al.*, 2016; Magalhães, 2020) have been found in 2nd and 1st century BC hillforts and sometimes earlier in Northwest Iberia. These are not abundant but testify to the consumption of the fruit before and during the early stages of Roman interaction in the region.

Seeds and fruits from wild species have been recovered in larger amounts, most likely related to the use of wood as fuel. This is most likely the case of seeds from heather (*Erica* sp.) and Fabaceae, the most abundant in the assemblage, whose wood has been identified in the charcoal analysis. Other species are likely weeds from the cereals but may also have been present in multiple ruderal contexts, pastures or simply bordering forest areas. *Polygonum amphibium* and *Polygonum lapathifolium*, whose achenes have been identified, are currently found in north-western Iberia in humid areas, next to streams or in irrigated fields (Villar, 1990).

Regarding wood charcoal, Alto da Raia revealed limited taxa diversity (tab. 1). The fuel used in the oven was mostly from shrubby Fabaceae, comprising most of the analysed fragments (84%). *Quercus* sp. type deciduous is also present with 7%, as well as residual evidence of *Cistus* sp. and *Erica* sp. The two remaining contexts, although providing less charcoal, displayed similar results. Given the spatial proximity between pit 302 and the oven and their similar charcoal results, it is likely that the charred contents of the former (probably an ash pit) originated from combustion events taking place in the latter.

Table 1. Anthracological and carpological data.

Context	Ditch	Pit	Oven		Total
SU	114	302	303	307	
Wood charcoal - taxa					
<i>Cistus</i> sp.	5	4			9
<i>Erica</i> sp.				2	2
Fabaceae	1	31	12	203	247
Fabaceae type <i>Adenocarpus</i>		5	5	61	71
Fabaceae type <i>Cytisus scoparius</i>		8		1	9
<i>Quercus</i> sp. type deciduous		2	9	20	30
Dycotiledon	11		3	8	22
Undetermined			1		1
Total - charcoal	17	50	30	295	391
Carpology - Cereals					
<i>Hordeum vulgare</i> subsp. <i>vulgare</i> (grain)			1	3	4
<i>Panicum miliaceum</i> (grain)			3	1	4
<i>Triticum</i> sp. (grain)			1		1
<i>Triticum</i> cf. <i>spelta</i> (glume base)			2		2
Triticeae (grain - frag.)				1	1
Carpology - Other taxa					
<i>Chenopodium</i> sp. (seed)				1	1
<i>Corrigiola</i> sp. (seed)			2	4	6
<i>Erica</i> sp. (seed)			22		22
Fabaceae - Genisteae type (seed)	2		5	3	10
<i>Ficus carica</i> (seed)				1	1
<i>Ornithopus</i> sp. (loment-frag.)				1	1
Poaceae (grain)				2	2
Polygonaceae (achene)				2	2
<i>Polygonum amphibium</i> (achene)				8	8
<i>Polygonum lapathifolium</i> (achene)				1	1
<i>Rumex acetosa</i> (achene)		1			1
<i>Rumex</i> sp. (achene)				1	1
<i>Trifolium</i> sp. (semente)			1	1	2
Undetermined - unit				2	2

Dendrological data obtained from these charcoal remains revealed extremely high percentages of strong tree ring curvatures (87,5%) across all taxa, suggesting not only the exploitation of shrubby taxa but also small branches of deciduous oak (tab. 2). Moreover, the number of fragments with vitrification (17%) and radial cracks (23%), mostly in Fabaceae, is not without relevance, particularly the latter which is usually associated with the burning of green wood (Thery-Parisot and Henry, 2012). The combined analysis of these results follows a pattern of wood use clearly in line with the type of short-span occupation of such temporary military sites. Wood procurement would have taken place in the immediate vicinity and availability would be its most likely driver since all taxa recorded are common in the region, particularly *Quercus robur* and *Quercus pyrenaica* and several shrubby Fabaceae from different genera (e.g., *Cytisus*, *Adenocarpus* and *Ulex*). However, the use of these scrubs in combination with larger and longer-lasting wood from *Quercus* is also a staple in regard of the fuelwood used in combustion structures throughout Northwest Iberia during this period.

Table 2. Dendrological data.

Taxon	Total ID	Tree-ring curvature			Radial cracks	Vitrification
		Strong	Moderate	Weak		
<i>Cistus</i> sp.	9	9			3	5
<i>Erica</i> sp.	2	2				1
Fabaceae	247	234	4	1	55	37
Fabaceae type <i>Adenocarpus</i>	71	70	1		16	10
Fabaceae type <i>Cytisus scoparius</i>	9	9			5	2
<i>Quercus</i> sp. type deciduous	31	16	1	3	4	4
Dicotelydon	22	2			9	9
Undetermined	1	1				

4.2. Geochemical studies of infill materials

Considering the defined SU and the textural changes along the infill sequence, small samples of around 10 g of material were collected through the cut section of trenches 1 and 2, to perform geochemical studies (tabs. 3 and 4). The samples were milled in agate mortars into a fine powder prior to the chemical and mineralogical analysis.

The chemical composition of the samples was obtained by using a lithium metaborate/tetraborate fusion with subsequent analysis by X-Ray Fluorescence (XRF), Inductively Coupled Plasma (ICP) and ICP/MS (Mass Spectrometry), performed at Activation Laboratories Ltd. (Actlabs, Canada: <http://www.actlabs.com>), using their standard analytical techniques and detection limits. The mineralogical composition was achieved by X-ray diffraction (XRD) using a Bruker D2 Phaser diffractometer equipped with a Cu-K α radiation X-ray tube (monochromatic radiation λ = 1.5406 Å). Non-oriented aggregate powders were prepared for the bulk material and scanned at 1° 2 θ /min, from 2-70° 2 θ . Diffractograms were compared with reference angle and intensity for identification of minerals (Brindley and Brown, 1980). Semi-quantitative analysis of mineral assemblages was undertaken to measure the principal peak areas with

intensities correction, using the recommended weighting factors (Schultz, 1964; Biscaye, 1965; Martin-Pozas, 1968; Trindade *et al.*, 2010). The mineralogical composition (additional data are given in Supplementary Material 1) fits the weathered granitic geological context (Martins and Ribeiro, 1979). Samples are mostly composed of quartz (26%-68%) and alkali feldspars (22%-67%). A lower proportion of phyllosilicates (2% - 33%), including micas and kaolin minerals was detected. Traces of plagioclases were also identified.

Table 3. Description of the samples collected at trench 1 for chemical and mineralogical studies, and luminescence dating (marked with*).

Samples from trench 1	Description		SU	Depth (cm)
AR1#16	Modern soil covering the ditch infill sequence and the embankment		100	5
AR1#15*	Embankment	Yellowish sandy sediment with contribution of weathering material from geological substrate	104	44
AR1#14*		Yellowish - brown sandy sediment with contribution of weathering material from geological substrate	111	64
AR1#13		Brownish-yellow sandy sediment, with contribution of weathering material from geological substrate	109	89
AR1#12	Ditch infill sequence	Brownish sandy sediment – at the same depth of the embankment bottom	102	12
AR1#11		Light brown sandy sediment with inclusions of roots and small quartz stones	105	60
AR1#10				75
AR1#9		Yellowish brown (darker at top) sandy sediment with contribution of weathering material from geological substrate	109	83
AR1#8*				91
AR1#7				105
AR1#6		Black sandy sediment	112	120
AR1#5		Brownish-yellow sandy sediment, with inclusions of small-sized quartz stones and dark and whitish spots		130
AR1#4		Whitish sandy sediment		145
AR1#3		Layer of black sandy sediment	114	157
AR1#2*		Brownish-yellow sandy sediment, with contribution of weathering material from geological substrate and black spots		183
AR1#1	Geological background - weathered granite – base of the ditch infill sequence and the embankment		106	190

Table 4. Description of the samples collected at trench 2 for chemical and mineralogical studies, and luminescence dating (marked with *).

Samples from Trench 2	Description		SU	Depth (cm)
AR2#10	Modern soil covering the ditch infill sequence		200	5
AR2#9	Ditch infill sequence	Dark brownish sandy sediment with some small quartz stones	201	35
AR2#8		2 nd moment of ditch infill - light brownish sandy sediment, with a great contribution of weathered granite and inclusions of roots and small quartz stones	203	63
AR2#7				80
AR2#6				100
AR2#5*		1 st moment of ditch infill - brownish sandy sediment, with a great contribution of weathered granite and inclusions of quartz stones	205	110
AR2#4				127
AR2#3				150
AR2#2*				160
AR2#1	Geological background - weathered granite – base of the ditch infill sequence		207	165

The mineralogical index of alteration (MIA) which evaluates the degree of mineralogical weathering, i.e. the transformation ratio of a primary mineral into its equivalent alteration mineral (Bahlburg and Dobrzinski, 2011). In this work, it was calculated by the ratio between the content of quartz and the content of all the silicates (quartz + feldspars) (Johnson, 1993; Haskins, 2006) so the high MIA values (27%<MIA<74%), point to a process of accumulation of locally sourced materials. In general, higher proportions of quartz and phyllosilicates are observed in samples subjected to weathering processes, tending to increase from the bottom towards the top of the infill sequences, with the highest MIA detected in modern soil and at the top of each infill phase. The discontinuity observed in the mineralogical proportions, as well as the MIA values, are good markers to establish distinct phases/moments/events in the infill of negative structures (Rodrigues *et al.*, 2013, 2019). It should be noted that, towards the top of the infill sequence at trench 1, high MIA levels (like soil) alternate with lower MIA levels (like the geological substrate), indicating a greater contribution of geological material in those infill levels. Based on the mineralogical composition, towards the top of trench 1, three main infill phases can be considered: i) a first phase comprising the materials from the bottom to about 100 cm of depth (SU 106, 114 and 112; tab. 3), more heterogeneous and with samples AR1#4 and AR1#6, whitish and black sandy distinct materials from SU 112; ii) a second phase containing materials between 100 cm and 20 cm of depth (SU 109 and 105; tab. 3), with an increase in the proportion of quartz and a decrease in feldspars, indicating a gradual increase in the weathering; iii) a final phase containing the materials collected at 12 cm of depth and the topsoil (SU 102 and 100; tab. 3), with the trend already identified in the previous phase. In the embankment, the mineralogical composition of materials sampled at 89 cm of depth is similar to the modern soil. Above this layer, the materials accumulated are similar to the geological substrate, being less weathered. This alteration in the expected sequence corroborates an inversion of the stratigraphy, which is consistent with the embankment formation processes, using material from the excavation

of the ditch. Similarly, at trench 2, the infill processes may have occurred in three phases: i) an initial infill phase, more heterogeneous and with a top layer including a higher clayed material content (at 110 cm of depth; SU 207 and 205; tab. 4); ii) a second phase between 110 cm and 35 cm of depth (SU 203 and 201; tab. 4), with a more homogeneous composition, with highly weathered materials; iii) a final phase containing material collected at 35 cm of depth and the modern soil (SU 201 and 200; tab. 4). The compositional variation along the sequence could point to an intentional selection of infill materials. The chemical element contents variations observed along the infill sequences and at the embankment (see Supplementary Material 1) enable to confirm the discontinuities already observed within the mineralogical composition. This corroborates the idea of a sequential infill, in which three phases are distinguished in the ditch of both trenches.

Multivariate statistical analysis was employed using the Statistica software (TIBCO Software Inc.) to compare the sampled materials with the chemical contents and the ‘loss on ignition’ (LOI) value as variables. The non-hierarchical clustering method (k-means) was applied to classify samples into a specified number of clusters (k) and emphasize the more relevant chemical elements for their distinction, enabling the associations between samples, especially between ones from the embankment and the upper infill phases of the trench 1. Four clusters were defined for samples from trench 1 (fig. 9). Cluster 1 includes samples collected at 91 cm (SU 109) and 75 cm (SU 105) of depth (second phase of infill) and the sample collected at 44 cm of depth (SU 104) at the embankment – samples had the lowest content of Si and the highest content of almost all chemical elements determined (with the exception of Ca, Na, V, Ba, Sr, Cu and Ta), as well as the highest content of organic matter (highest LOI) Cluster 2 comprises samples collected at 105 cm (SU 109) of depth (corresponding to the top of the first phase) and those from 83 cm (SU 109) and 60 cm (SU 105) of depth (second phase of infill), 12 cm of depth (SU 102) and modern soil (SU 100) (final phase) and samples collected at 89 cm (SU 109) and 64 cm (SU 111) of depth at the bottom of the embankment – samples with the lowest content of Ba, Sr and Eu. Cluster 3 contain the sample of geological background (SU 106) and samples collected at 183 cm (SU 114) and 130 cm (SU 112) of depth (first phase of infill) - these samples have the lowest contents of Ca, Na, Ti, P, V, Y, Zr, Sn, Cs, REE, Hf, Ta, W, Th, U and organic matter (lowest LOI). Cluster 4 consists of three detachable samples, collected at the first phase of infill - at 157 cm of depth (SU 114; layer of black sandy sediment), at 145 cm of depth (SU 112; whitish sandy sediment) and at 120 cm of depth (SU 112; black sandy sediment) - samples with the highest content of Si, Ca, Na, Ba, Sr and Ta and the lowest content of Al, Fe, Mn, K, Co, Cu, Zn, As, Rb, Tl and Pb. The multivariate analysis, based on the chemical composition of the samples, allowed: on the one hand, to identify the similarity of some infilling materials with the local geological material, revealing the high contribution of the latter in the ditch infilling process; on the other hand, it enabled to associate the infilling materials with the embankment materials, corroborating that the infilling of the ditch may have occurred due to the collapse of the embankment, especially between the end of the first phase and the second phase.

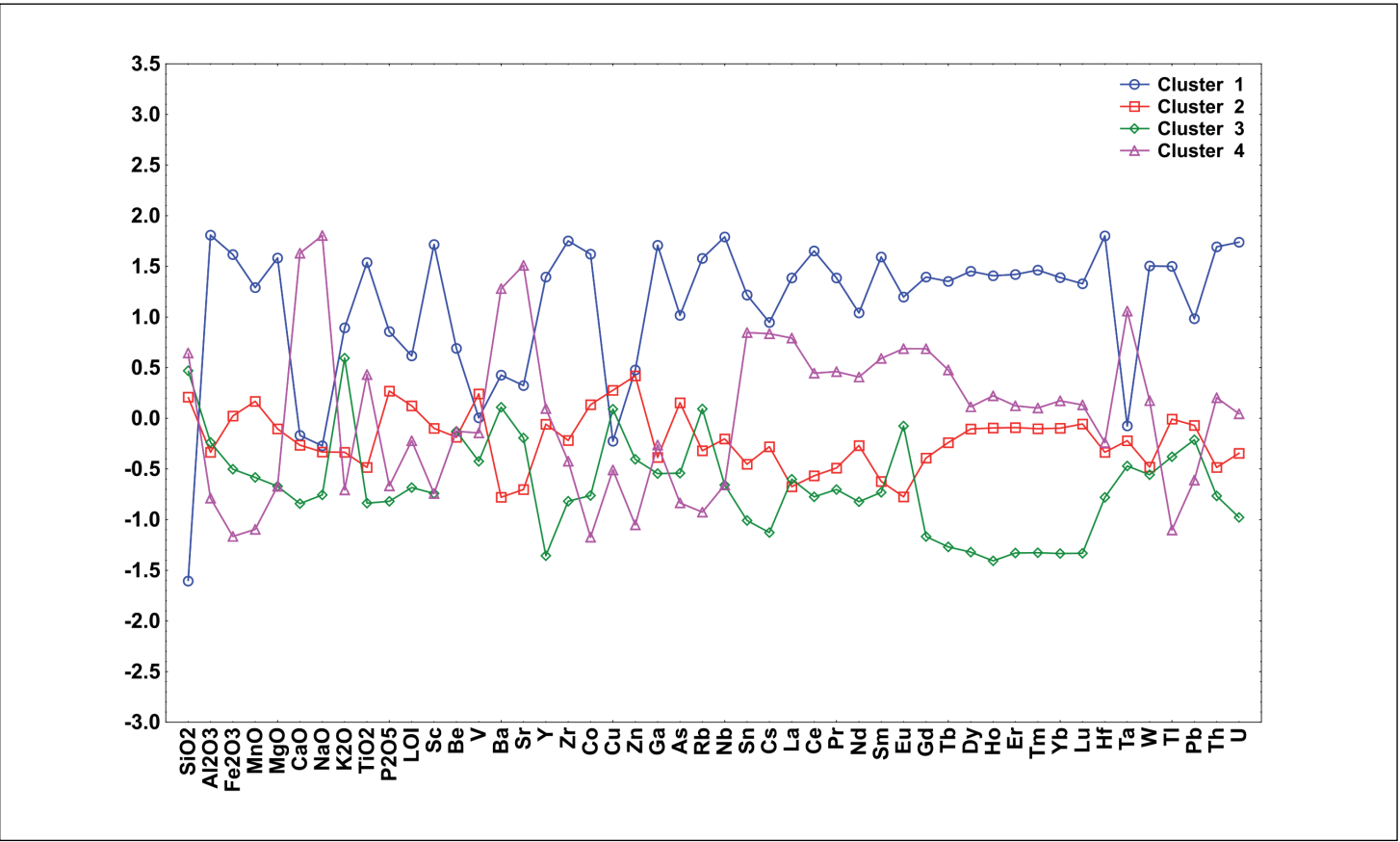


Figure 9. Plot of means for each cluster (k-means method) for samples from trench 1, using chemical results of chemical analysis as variables.

4.3. Absolute dating

4.3.1. Radiocarbon dating

The radiocarbon dates were calibrated using the program OxCal 4.4 (Bronk Ramsey, 2009) and the IntCal 20 calibration curve (Reimer *et al.*, 2020). Three samples were collected for radiocarbon dating: one charcoal in the fifth filling layer (SU 114) of the ditch in trench 1 (AR.S1.114.01) where a concentration of burned material was identified, and two charred barley seeds from the infill of the oven in trench 3 (AR.S3.307.01 and AR.S3.307.02). Assuming the oven is contemporary with the camp given its location strictly within its southeast corner, the calibrated dates of samples AR.S3.307.01 [48 cal BC – 80 cal AD] and AR.S3.307.02 [47 cal BC – 72 cal AD] point to a probable occupation of the site between the second half of the 1st century BC and the first half of the 1st century AD (fig. 10). The calibrated date of sample AR.S1.114.01 [368 cal BC – 173 cal BC] is more likely to be related to an Iron Age activity on site and was mixed with the filling material of the ditch (fig. 10).

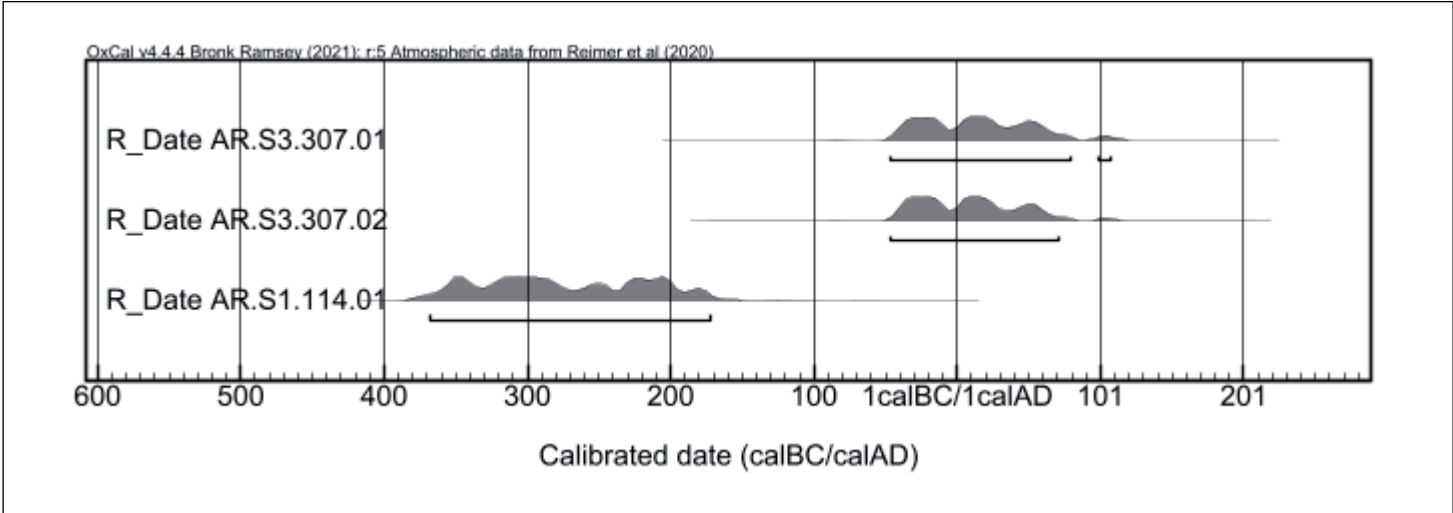


Figure 10. Calibrated radiocarbon dates.

4.3.2. Luminescence dating

At trenches 1 and 2, samples (AR1#2, AR1#8, AR1#14, AR1#15, AR2#2, AR2#5) from selected deposits of accumulated material (tabs. 3 and 4) were collected for absolute dating by luminescence protocols. These samples were chosen to obtain the luminescence age of the materials considered, at the time of excavation, as the most relevant for understanding the dynamics of the ditch filling and the formation of the embankment. Six samples of around 500 g were collected by using stainless steel tubes for the luminescence age of the most relevant materials deposited, avoiding sunlight exposure. *In situ* field gamma spectrometry was performed in the sampling holes in order to obtain the environmental K, Th and U contents, crucial to dose rate calculation. Absolute dating by using luminescence techniques implies the use of chemical and dosimetry measurements, considering the luminescence age equation:

$$\text{Luminescence Age (ka)} = \text{Absorbed Dose (Gy)} / \text{Dose Rate (Gy/ka)}.$$

The absorbed dose (De) was obtained by dosimetry, applying luminescence protocols and represents the laboratory dose of radiation (accumulated energy) needed to induce ‘artificial’ luminescence equal to the natural signal (Aitken, 1999). The laboratory procedures

for the preparation of a quartz coarse grains fraction of samples were performed following the suggestion by Rodrigues *et al.* (2013, 2019). Quartz purity check (Duller, 2003) and the dose recovery test (Murray and Wintle, 2003) were conducted, and luminescence quantitative measurements were performed using a SAR-OSL (Single Aliquot Regenerative-Optically Stimulated Luminescence) protocol with an internal pre-heat test (Murray and Wintle, 2000). Forty-eight aliquots were measured using Risø readers DA-20 equipped with a $^{90}\text{Sr}/^{90}\text{Y}$ beta source delivering $0,072 \pm 0.002 \text{ Gys}^{-1}$ (Risø reader 1 – Sample AR1#15) or $0.107 \pm 0.00 \text{ Gys}^{-1}$ (Risø reader 3 - AR1#2, AR1#8, AR1#14, AR2#2, AR2#5) with Hoya U-340 detection filter. The accepted results following the criteria described in Rodrigues *et al.* (2022) and Eixea *et al.* (2023) were analysed statistically to estimate the absorbed dose for the sample using the robust mean and the respective uncertainty calculated by Robust Statistics V1.0. The dose rate (Dr) was estimated by using a conventional protocol (as described in Rodrigues *et al.* 2019) and included alpha, beta, gamma and cosmic radiation, based on chemical analyses and dosimetry measurements and defines the rate at which energy is absorbed from the flux of nuclear radiation. It was evaluated by assessment of the radioactivity of the sample and its surrounding burial material. This was carried out both in the laboratory (chemical analyses and estimative of cosmic radiation) and in the field (*in situ* gamma spectrometry) (Aitken, 1999; Burbidge *et al.*, 2014; Marques *et al.*, 2021). The dose rate was corrected to the water content and granulometry of the studied material (Odriozola *et al.*, 2014; Rodrigues *et al.*, 2019).

The content of K, Th and U obtained *in situ* by gamma spectrometry are on average 3.1%, 6.3 mg/kg and 4.8 mg/kg, respectively (tab. 5). Considering the chemical analysis performed, the average chemical contents of K, Rb, Th and U are 4.6%, 185 mg/kg, 10.1 mg/kg, and 6.6 mg/kg, respectively. The estimated water content during the burial time ranges between 13% and 30%. The dose rate average obtained is 5.6 Gy/ka. Considering the results of the quartz purity (OSL/IRSL depletion ratio around 1) and recovery dose tests (in the range of 0.98-1.10), a quantitative SAR-OSL protocol was applied for the determination of De. The robust mean of the results obtained for all samples ranges between 12.8 Gy and 48.7 Gy, with uncertainties between 1% and 4%. The uncertainties are a consequence of the dispersion of the absorbed dose within each sample. The luminescence ages of the samples were calculated and ranged between 2.15 ka and 7.3 ka, with uncertainties between 4% and 9%.

The materials accumulated in the ditch, and sampled for luminescence dating, comprise a portion of weathered geological material, in a non-negligible amount. The compositional analyses confirmed this contribution of geological material in the infill layers. Thus, the luminescence ages obtained must be affected by the presence of this geological material, especially sample AR1#15, collected at the bottom of the embankment. The analysed material was not adequately exposed to sunlight (incomplete bleaching) before deposition in the ditch, probably because of rapid events which mixed more superficial and exposed materials with fragments of geological material. As such, a residual geological dose is preserved in the quartz grains, leading to an overestimation of the absorbed dose (De) and, consequently, of the luminescence age. Although overestimated, the ages obtained are stratigraphically consistent with each other (luminescence ages decrease upwards) within each trench, as well as with the radiocarbon date obtained for the material collected in trench 1 (SU 114). An aspect to note is the inversion of the luminescence ages obtained for samples from the embankment, pointing to an inversion of stratigraphy, as already suggested by the compositional studies. This is in accordance with the construction of this structure with geological material taken from the ditch.

Table 5. Chemical content of K, Tb, Th and U determined by chemical and dosimetric analyses, water contents, dose rate (Dr) and absorbed dose (De) determined by luminescence for coarse quartz grains and luminescence ages.

Sample			AR1#2	AR1#8	AR1#14	AR1#15	AR2#2	AR2#5
SU			114	109	111	104	205	205
In situ gamma spectrometry	K	%	3.17	3.16	3.20	3.15	3.30	2.88
		±	0.04	0.04	0.04	0.04	0.04	0.04
	Th	mg/kg	4.70	4.71	4.80	4.69	4.72	5.09
		±	0.44	0.44	0.44	0.44	0.44	0.47
	U	mg/kg	6.47	6.50	6.48	6.52	5.03	6.72
		±	0.63	0.63	0.63	0.63	0.50	0.65
FUS-ICP	K	%	4.43	5.56	4.33	5.12	4.47	3.96
		±	0.01	0.01	0.01	0.01	0.01	0.01
FUS-MS	U	mg/kg	4.8	8.3	5	9.6	5.2	6.5
		±	0.1	0.1	0.1	0.1	0.1	0.1
	Th	mg/kg	7.4	12.6	7.2	18.1	5.4	9.9
		±	0.1	0.1	0.1	0.1	0.1	0.1
	Rb	mg/kg	160	205	158	201	175	212
		±	2	2	2	2	2	2
Water Content		%	16	13	13	13	13	30
Dr		Gy/ka	5.1	6.6	5.3	6.7	5.2	4.6
		±	0.2	0.2	0.2	0.2	0.2	0.2
De		Gy	14.8	14.2	14.8	48.7	15.5	12.8
		±	0.6	0.1	0.4	4.1	0.5	0.4
Luminescence Age		ka	2.9	2.15	2.8	7.3	3.0	2.8
		±	0.1	0.06	0.1	0.6	0.1	0.1
	cy	(BC)	980 - 780	190 - 70	880 - 680	5880 - 4680	1080 - 880	880 - 680

4.4. Material culture

Roman military sites with temporary occupations are notoriously limited in material culture and this site was no exception (Peralta Labrador, 2002; Fonte *et al.*, 2023). The metal detector survey on the modern path allowed some recent metal rubbish to be recovered, but also two hobnails of probable military origin, albeit in a poor state of preservation. Regarding pottery, only a few small-scale ceramic sherds were recovered, 21 in total, one rim, and twenty wall fragments (tab. 6). The classification and description of the ceramic fragments were based on the regional analytical criteria for the Bronze Age pottery of Bettencourt (1999) and for the Iron Age pottery of Martins (1987, 1990). The fragmentation study criteria of Brudenell and Cooper (2008) was also applied, enabling to relate the level of fragmentation and erosion rates of ceramics with the depositional and post-depositional phenomena. Aspects such as shape, production form, firing conditions, paste, non-plastic elements (NPE) and surface treatments of these fragments were considered, alongside the degree of erosion and use over fire (presence of soot). Accordingly, most of the ceramic fragments analysed are small (less than 4 cm), except for two larger fragments between 4 and 8 cm in size (SU 201 and SU 206). In addition to the strong fragmentation, the ceramic sherds present significant erosion suggesting that they were affected by depositional and post-depositional processes for a considerable time.

Although the ceramic fragments are too small to reveal their form or function, their technical-morphological analysis points to two main different production contexts. A first, older production context is characterised by medium to coarse textured pots with sandy-micaceous and sandy paste, produced under reducing fire conditions, with medium/large NPE. The surface of these pots was mostly smoothened, though three of them had been polished. This is followed by a second, more recent production context, characterized by vessels of medium to fine texture made of micaceous paste with small NPE and produced under oxidizing fire conditions and with smoothened surfaces.

The technical and formal characteristics of these ceramics seem to indicate that they were produced prior to the Roman occupation. We can separate them into two productions, most likely pre-Roman: the first group appears to be a production that we can generally place in the Bronze Age and the second group generally dated from the Iron Age. As no structures or other materials were found, for example imported, it is quite difficult to determine whether or not this site was occupied before the Roman period.

Considering that these materials were found in the context of their last deposition and therefore in a secondary context, it must be assumed that the ceramic fragments do not have a direct chronological link with the structures and contexts found, namely the defensive enclosure and its oven. Several anomalies detected in the magnetic survey seem to be related to these prehistoric occupations (fig. 3, B and C). However, this still needs further investigation.

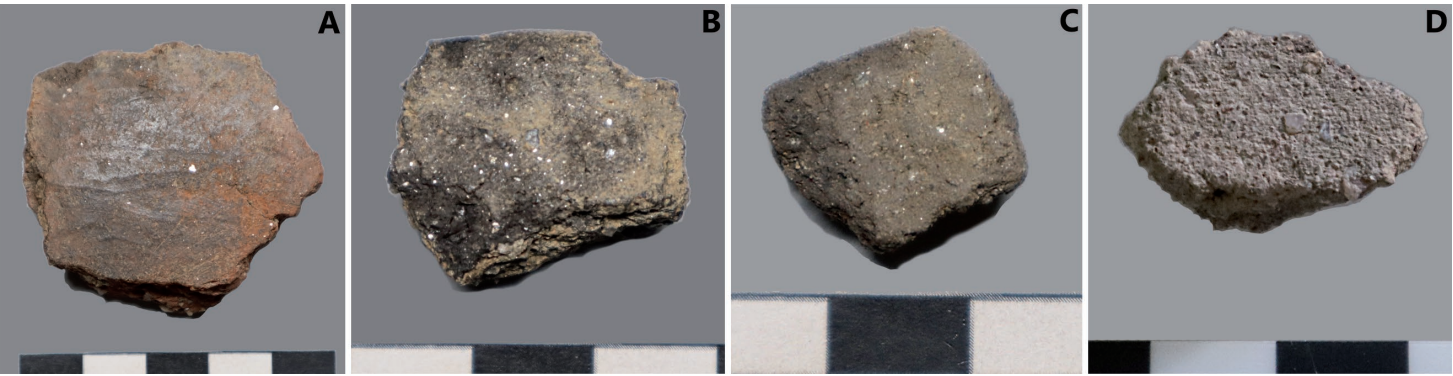


Figure 11. Bronze Age (A and B) and Iron Age (C and D) ceramic fragments.

Table 6. Chronology of the ceramic fragments from each trench.

Chronology	Trench 1			
	SU 103	SU 104	SU 107	SU 111
Bronze Age	1	4	1	2
Iron Age	–	1	–	1
	Trench 2			
	SU 201	SU 202	SU 203	SU 206
Bronze Age	3	1	3	3
Iron Age	–	–	–	–
	Trench 3			
	SU 303			
Bronze Age	–			
Iron Age	1			

5. DISCUSSION AND CONCLUSIONS

The results of this interdisciplinary and multi-proxy approach seem to indicate that the Alto da Raia enclosure was a Roman military camp that was probably occupied between the second half of the 1st century BC and the first half of the 1st century AD. The location, morphology, defensive system, absolute dating, and some of the material culture recovered, support this hypothesis. The data suggests that the camp was possibly abandoned gradually, or at least its abandonment did not imply its complete destruction. The ditch seems to have been filled sequentially and selectively and the embankment was not entirely thrown into the ditch, which only happened after the ditch was already half full. This indicates that the embankment, built with geological material taken from the ditch, might have collapsed by natural erosion rather than by human action.

However, the camp probably overlapped previous prehistoric activity on site in the Bronze Age and in the Iron Age. Research into these contexts needs to be further developed in order to establish their nature and extent.

The function of this Roman temporary camp is less evident as it does not seem to be directly related to military campaigning. Due to its exposed location and the fact that it is surrounded by several Iron Age hillforts, it does not seem to have been related to conquest wars. Perhaps it was related instead to a context of territorial reorganization and resource exploitation that occurred immediately after the end of the conquest and integration of this area into the Roman Empire at the end of the 1st century BC under *Augustus* (González-Álvarez *et al.*, 2019; Morillo *et al.*, 2020; Fonte, 2022). If so, this raises interesting questions regarding potential diplomatic interactions between the Roman army and the indigenous communities that inhabited this area which requires further research. The indigenous communities of this area were probably actively involved with the Roman army in the exchange of various products and materials, including the transfer of know-how and different practices, as the material evidence recovered from several nearby Late Iron Age hillforts seems to point out. The Alto da Raia Roman camp is in the same chronological horizon as several indigenous and Roman sites, both military and civilian, in Northwest Iberia that were directly related to the restructuring of this territory operated by Rome after the Cantabrian Wars (29-19 BC) that ended the long conquest process of *Hispania* (Peralta Labrador *et al.*, 2019; Morillo *et al.*, 2020).

This camp fits into “group 2: medium-sized temporary camps” (Costa-García *et al.*, 2019, pp. 25-30) that might have housed “several thousand men (*ca.* 2000-4000) (...), [and] they reveal the enormous operative versatility of the Roman army when deploying *vexillationes* (detachments) with major tactical autonomy.” (*op. cit.*: 24). These medium-sized camps were possibly related with this initial phase of Roman post-conquest territorial reorganization and resource exploitation in Northwest Iberia.

Appendix

Chemical and mineralogical composition of the samples.

<https://revistascientificas.us.es/index.php/spal/article/view/25208/22468>

Acknowledgments

J.F. was funded by a Marie Skłodowska-Curie Individual Fellowship “Finisterrae: Negotiating and contesting marginal landscapes on the Western fringes of the Roman Empire” funded under the European Union’s Horizon 2020 research and innovation programme under the Marie Skłodowska-Curie grant agreement No 794048.

Part of this research was also funded by FEDER through the COMPETE 2020 Programme, Lisboa Regional Programme and European Regional Development Fund (FEEI), and National Funds through FCT (Fundação para a Ciência e a Tecnologia) under the scope of the Iberian Tin project (PTDC/HAR-ARQ/32290/2017).

We acknowledge the grant from The Roman Society through their Donald Atkinson Fund which provided additional funding for absolute dating.

C2TN/IST authors gratefully acknowledge the FCT (Portuguese Science and Technology Foundation) support through the UID/Multi/04349/2020 and post-doctoral grant SFRH/BPD/114986/2016 of A. L. R.

N.O. is grateful for the FCT PhD Grant (SFRH/BD/138105/2018) whose funding was guaranteed by national funds from the Ministry of Science, Technology and Higher Education of the Portuguese Government but also by the European Social Fund (ESF), through the Regional Operational Programme North 2020 and POCH - Human Capital Operational Programme.

The archaeological survey at Alto da Raia was funded by the Montalegre and Calvos de Randín Municipalities and done in collaboration with the Era-Arqueologia company. We are also thankful to the Junta de Freguesia de Tourém, the Conselho Diretivo dos Baldios de Tourém and the Calvos de Randín Municipality for their help with the vegetation clearance of the site.

We would like to thank João Hipólito from Era-Arqueologia for his help with the drawings of the archaeological excavation.

Special thanks are due to Rebeca Blanco-Rotea for bringing this site to our attention.

Authors’ contributions

- Conception and design: JF.
- Archaeological excavation: JF, TP, FR, VC, JC, CJ.
- Data collection: JF, JPT, ALR, TP, JGS, JAG, EM.
- Data analysis and interpretation: JF, JPT, ALR, TP, JAG, JGS.
- Laboratory and statistical analysis: JPT, FCV, ALR, MID, RM, DR, PM, MCR, NO.
- Drafting: JF, JPT, ALR, JGS, NO.
- Critical revision of the text: JF, JPT, ALR, JGS, MG, JC, EM, IO.
- Graphic design: JF, FR, VC, CJ.

REFERENCES

- Aitken, M. (1999) “Archaeological dating using physical phenomena”, *Reports on Progress in Physics*, 62, pp. 1333-1376. <https://doi.org/10.1088/0034-4885/62/9/202>
- Anderberg, A. L. (1994) *Atlas of seeds and small fruits of Northwest-European plant species with morphological descriptions*. Stockholm: Swedish Museum of Natural History.
- Arabaolaza, I. (2019) “A Roman Marching Camp in Ayr”, *Britannia*, 50, pp. 330-349. <https://doi.org/10.1017/S0068113X19000059>

- Armada, X. L. and García-Vuelta, O. (2015) "Dating Iron Age goldwork: First direct AMS 14C results from Northwestern Iberia", *Trabajos de Prehistoria*, 72(2), pp. 272-282. <https://doi.org/10.3989/tp.2015.12160>
- Armada, X. L. and García-Vuelta, O. (2021) "Plano-convex ingots and precious metalwork in northwestern Iberia during the Late Iron Age and early Roman period: An analytical approach", *Archaeological and Anthropological Sciences*, 13(78). <https://doi.org/10.1007/s12520-021-01323-2>
- Bahlburg, H. and Dobrzinski, N. (2011) "A review of the Chemical Index of Alteration (CIA) and its application to the study of Neoproterozoic glacial deposits and climate transitions", in Arnaud, E., Halverson, G.P. and Shields, G.A. (eds.) *The Geological Record of Neoproterozoic Glaciations*, 36. London: Geological Society of London, pp. 81-92. <https://doi.org/10.1144/M36.6>
- Bettencourt, A. M. S. (1999) *A Paisagem e o Homem na bacia do Cávado durante o II e o I milénios AC*. PhD thesis. Universidade do Minho. (Available at <https://hdl.handle.net/1822/83209>, accessed on November 2023).
- Biscaye, P.E. (1965) "Mineralogy and sedimentation of recent deep-sea clay in the Atlantic Ocean and adjacent seas and oceans", *Geological Society of America Bulletin*, 76, pp. 803-832.
- Brindley, G.W. and Brown, G. (1980) *Crystal structures of clay minerals and their X-ray identification*. London: Mineralogical Society.
- Bronk Ramsey, C. (2009) "Bayesian Analysis of Radiocarbon Dates", *Radiocarbon*, 51(1), pp. 337-360. <https://doi.org/10.1017/S0033822200033865>
- Brudenell, M. and Cooper, A. (2008) "Post-middenism: depositional histories on later Bronze Age settlements at Broom, Bedfordshire", *Oxford Journal of Archaeology*, 27, pp. 15-36. <https://doi.org/10.1111/j.1468-0092.2007.00293.x>
- Burbidge, C. I., Trindade, M. J., Dias, M. I., Oosterbeek, L., Scarre, C., Rosina, P., Cruz, A., Cura, S., Cura, P., Caron, L., Prudêncio, M. I., Cardoso, G. J. O., Franco, D., Marques, R. and Gomes, H. (2014) "Luminescence dating and associated analyses in transition landscapes of the Alto Ribatejo, Central Portugal", *Quaternary Geochronology*, 20, pp. 65-77. <https://doi.org/10.1016/j.quageo.2013.11.002>
- Cavallo, C., Kooistra, L. I. and Dütting, K. K. (2008) "Food supply to the Roman army in the Rhine delta in the first century A.D.", in Stallibrass, S. and Thomas, R. (eds.) *Feeding the Roman Army: The Archaeology of Production and Supply in NW Europe*. Oxford: Oxbow Books, pp. 69-82.
- Centeno, R. (2011) "Da República ao Império: Reflexões sobre a monetização no ocidente da Hispania", in García-Bellido, M. P., Callegarin, L. and Jiménez, A. (eds.) *Barter, Money and Coinage in the Ancient Mediterranean (10th-1st Centuries BC)*. Madrid: CSIC, pp. 355-367.
- Costa-García, J. M., Fonte, J. and Gago, M. (2019) "The reassessment of the Roman military presence in Galicia and northern Portugal through digital tools: archaeological diversity and historical problems", *Mediterranean Archaeology and Archaeometry*, 19(3), pp. 17-49. <https://doi.org/10.5281/zenodo.3457524>
- Doneus, M. (2013) "Openness as Visualization Technique for Interpretative Mapping of Airborne Lidar Derived Digital Terrain Models", *Remote Sensing* 5, pp. 6427-6442. <https://doi.org/10.3390/rs5126427>
- Duller, G. (2003) "Distinguishing quartz and feldspar in single grain luminescence measurements", *Radiation Measurements*, 37, pp. 161-165. [https://doi.org/10.1016/S1350-4487\(02\)00170-1](https://doi.org/10.1016/S1350-4487(02)00170-1)
- Eguileta Franco, J. M. (2003) *Mámoas y paisaje, muerte y vida en Val de Salas (Ourense): el fenómeno megalítico en un valle de montaña*. Vigo: Universidade de Vigo.
- Eixea, A., Bel, M. Á., Carrión, Y., Ferrer-García, C., Guillem, P. M., Martínez-Alfaro, A., Martínez-Varea, C. M., Moya, R., Rodrigues, A. L., Dias, M. I., Russo, D. and Sanchis, A. (2023) "A multi-proxy study from new excavations in the Middle Palaeolithic site of Cova del Puntal del Gat (Benirredrà, València, Spain)", *Comptes Rendus Palevol*, 22(10), pp. 159-200. <https://doi.org/10.5852/cr-palevol2023v22a10>
- Figueiral, I. (1990) *Le Nord-Ouest du Portugal et les modifications de l'écosystème, du Bronze final à l'époque romaine, d'après l'anthracanalyse de sites archéologiques*. PhD thesis. Université des Sciences et Techniques du Languedoc.
- Figueiredo, E., Rodrigues, A., Fonte, J., Meunier, E., Dias, F., Lima, A., Gonçalves, J. A., Gonçalves-Seco, L., Gonçalves, F., Pereira, M. F. C., Silva, R. J. C. and Veiga, J.P. (2022) "Tin and Bronze

- Production at the Outeiro de Baltar Hillfort (NW Iberia)", *Minerals*, 12(6), 758. <https://doi.org/10.3390/min12060758>
- Fonte, J. (2022) "Late Iron Age and early Roman conflict and interaction in southern *Callaecia* (north-west Iberia)", in Stek, T. D. and Carneiro, A. (eds.) *The Archaeology of Roman Portugal in its Western Mediterranean Context*. Oxford: Oxbow Books, pp. 27-46.
- Fonte, J., Costa-García, J. M. and Gago, M. (2022) "O Penedo dos Lobos: Roman military activity in the uplands of the Galician Massif (Northwest Iberia)", *Journal of Conflict Archaeology*, 17(1), pp. 5-29. <https://doi.org/10.1080/15740773.2021.1980757>
- Fonte, J., Rodrigues, A. L., Dias, M. I., Russo, D., Pereiro, T., Carvalho, J., Amorim, S., Jorge, C., Monteiro, P., Ferro-Vázquez, C., Costa-García, J.M., Gago, M. and Oltean, I. (2023) "Reassessing Roman military activity through an interdisciplinary approach: Myth and archaeology in Laboreiro Mountain (Northwestern Iberia)", *Journal of Archaeological Science: Reports*, 49, 103993. <https://doi.org/10.1016/j.jasrep.2023.103993>
- García Sánchez, J., Costa-García, J. M., Fonte, J. and González-Álvarez, D. (2022) "Exploring Ephemeral Features with Ground-Penetrating Radar: An Approach to Roman Military Camps", *Remote Sensing* 14, 4884. <https://doi.org/10.3390/rs14194884>
- González-Álvarez, D., Costa-García, J. M., Menéndez-Blanco, A., Fonte, J., Álvarez-Martínez, V., Blanco-Rotea, R. and Gago, M. (2019) "La presencia militar romana en el noroeste ibérico hacia el cambio de era: estado actual y retos de futuro", in Vallori Márquez, B., Rueda Galán, C. and Bellón Ruiz, J. P. (eds.) *Accampamenti, guarnigioni e assedi durante la Seconda Guerra Punica e la conquista romana (secoli III-I a.C.): prospettive archeologiche*. Roma: Edizioni Quasar, pp. 127-138.
- Haskins, D. (2006) *Chemical and mineralogical weathering indices as applied to a granite saprolite in South Africa*. IAE2006 Paper number 465. London: The Geological Society of London.
- Hesse, R. (2010) "LiDAR-derived Local Relief Models – a new tool for archaeological prospection", *Archaeological Prospection*, 17, pp. 67-72. <https://doi.org/10.1002/arp.374>
- Howland, M. D., Tamberino, A., Liritzis, I. and Thomas, E. L. (2022) "Digital Deforestation: Comparing Automated Approaches to the Production of Digital Terrain Models (DTMs) in Agisoft Metashape", *Quaternary*, 5(1), 5. <https://doi.org/10.3390/quat5010005>
- Johnson, M.J. (1993) "The system controlling the composition of clastic sediments", in Johnsson, M.J. and Basu, A. (eds.) *Processes controlling the composition of clastic sediments*. Geological Society of America Special Paper, 285, pp. 1-19. <https://doi.org/10.1130/SPE284-p1>
- Kenney, J. and Parry, L. (2012) "Excavations at Ysgol yr Hendre, Llanbeblig, Caernarfon: a possible construction camp for *Segontium* fort and early medieval cemetery", *Archaeologia Cambrensis*, 161, pp. 249-284. <https://doi.org/10.5284/1059189>
- Kokalj, Ž. and Somrak, M. (2019) "Why Not a Single Image? Combining Visualizations to Facilitate Fieldwork and On-Screen Mapping", *Remote Sensing*, 11(7), 747. <https://doi.org/10.3390/rs11070747>
- Lorenzo Fernández, J. (1970). "Tesorillo protohistórico de Calvos de Randín", *Archivo Español de Arqueología*, 43, pp. 228-232.
- Magalhães, C. (2020) *Achas na Fogueira. Estudo antracológico do Castro de Guifões (Matosinhos)*. MSc thesis. Faculdade de Letras da Universidade do Porto. (Available at <https://hdl.handle.net/10216/131415>, accessed on November 2023).
- McParland, L. C., Collinson, M. E., Scott, A.C., Campbell, G. and Veal, R. (2010) "Is vitrification in charcoal a result of high temperature burning of wood?", *Journal of Archaeological Science*, 37, pp. 2679-2687. <https://doi.org/10.1016/j.jas.2010.06.006>
- Marguerie, D. and Hunot, J. Y. (2007) "Charcoal analysis and dendrology: data from archaeological sites in north-western France", *Journal of Archaeological Science*, 34, pp. 1417-1433. <https://doi.org/10.1016/j.jas.2006.10.032>
- Marques, R., Prudêncio, M. I., Russo, D., Cardoso, G., Dias, M. I., Rodrigues, A. L., Reis, M., Santos, M. and Rocha, F. (2021) "Evaluation of naturally occurring radionuclides (K, Th and U) in volcanic soils from Fogo Island, Cape Verde", *Journal of Radioanalytical and Nuclear Chemistry*, 330, pp. 347-355. <https://doi.org/10.1007/s10967-021-07959-7>

- Martín-Pozas, J. M. (1968) *El análisis mineralógico cuantitativo de los filosilicatos de la arcilla por difracción de rayos X*. PhD thesis. Universidad de Granada.
- Martins, M. (1987) “A cerâmica proto-histórico do vale do Cávado: tentativa de sistematização” *Cadernos de Arqueologia*, 4, pp. 35-77.
- Martins, M. (1990) *Povoamento proto-histórico e a romanização da bacia do curso médio do Cávado*. Cadernos de Arqueologia - Monografias 5. Braga: Unidade de Arqueologia da Universidade do Minho.
- Martins, J. A. and Ribeiro, M. L. (1979) *Notícia Explicativa da Folha 2-C Tourém. Carta Geológica de Portugal na escala de 1/50000*. Lisboa: Direcção-Geral de Geologia e Minas, Serviços Geológicos de Portugal.
- Morillo, Á., Adroher, A., Dobson, M. and Martín Hernández, E. (2020) “Constructing the archaeology of the Roman conquest of Hispania: new evidence, perspectives and challenges”, *Journal of Roman Archaeology*, 33, pp. 36-52. <https://doi.org/10.1017/S1047759420000902>
- Murray, A. S. and Wintle, A. G. (2000) “Luminescence dating of quartz using an improved single-aliquot regenerative-dose protocol”, *Radiation Measurements*, 32, pp. 57-73. [https://doi.org/10.1016/S1350-4487\(99\)00253-X](https://doi.org/10.1016/S1350-4487(99)00253-X)
- Murray, A. S. and Wintle, A. G. (2003) “The single aliquot regenerative dose protocol: Potential for improvements in reliability”, *Radiation Measurements*, 37, pp. 377-381. [https://doi.org/10.1016/S1350-4487\(03\)00053-2](https://doi.org/10.1016/S1350-4487(03)00053-2)
- Neef, R., Cappers, R. and Bekker, R. (2012) *Digital atlas of economic plants in archaeology*. Groningen: Barkhuis and Groningen University Library.
- Odriozola, C. P., Burbidge, C. I., Dias, M. I. and Hurtado, V. (2014) “Dating of Las Mesas Copper Age walled enclosure (La Fuente, Spain)”, *Trabajos de Prehistoria*, 71, pp. 343-352. <https://doi.org/10.3989/tp.2014.12138>
- Peña-Chocarro, L., Pérez- Jordà, G., Alonso, N., Antolín, F., Teira-Brión, A., Tereso, J. P., Montes Moya, E. M. and López Reyes, D. (2019) “Roman and medieval crops in the Iberian Peninsula: A first overview of seeds and fruits from archaeological sites”, *Quaternary International*, 499, pp. 49-66. <https://doi.org/10.1016/j.quaint.2017.09.037>
- Peralta Labrador, E. (2002) “Los campamentos romanos de campaña (*castra aestiva*): evidencias científicas y carencias académicas”, *Nivel Cero: revista del grupo arqueológico Attica*, 10, pp. 49-87.
- Peralta Labrador, E., Camino Mayor, J. and Torres-Martínez, J. F. (2019) “Recent research on the Cantabrian Wars: the archaeological reconstruction of a mountain war”, *Journal of Roman Archaeology*, 32, pp. 421-438. <https://doi.org/10.1017/S1047759419000217>
- Puente, I., Solla, M., Lagüela, S. and Sanjurjo-Pinto, J. (2018) “Reconstructing the Roman site “Aquis Querquennis” (Bande, Spain) from GPR, T-LiDAR and IRT data fusion”, *Remote Sensing*, 10(3), 379. <https://doi.org/10.3390/rs10030379>
- Reimer, P.J., Austin, W.E.N., Bard, E., Bayliss, A., Blackwell, P.G., Bronk Ramsey, C., Butzin, M., Cheng, H., Edwards, R.L., Friedrich, M., Grootes, P.M., Guilderson, T.P., Hajdas, I., Heaton, T.J., Hogg, A.G., Hughen, K.A., Kromer, B., Manning, S.W., Muscheler, R., Palmer, J.G., Pearson, C., van der Plicht, J., Reimer, R.W., Richards, D.A., Scott, E.M., Southon, J.R., Turney, C.S.M., Wacker, L., Adophi, F., Büntgen, U., Capano, M., Fahrni, S., Fogtmann-Schulz, A., Friedrich, R., Kudsk, S., Miyake, F., Olsen, J., Reinig, F., Sakamoto, M., Sookdeo, A., Talamo, S. (2020) “The IntCal20 Northern Hemisphere Radiocarbon Age Calibration Curve (0–55 cal kBP)” *Radiocarbon*, 62(4), pp. 725-757. <https://doi.org/10.1017/RDC.2020.41>
- Rodrigues, A. L., Burbidge, C. I., Dias, M. I., Rocha, F., Valera, A. C. and Prudêncio, M. I. (2013) “Luminescence and mineralogy of profiling samples from negative archaeological features”, *Mediterranean Archaeology and Archaeometry*, 13(3), pp. 37-47.
- Rodrigues, A.L., Dias, M. I., Valera, A. C., Rocha, F., Prudêncio, M. I., Marques, R., Cardoso, G. and Russo, D. (2019) “Geochemistry, luminescence and innovative dose rate determination of a Chalcolithic calcite-rich negative feature”, *Journal of Archaeological Science: Reports*, 26, 101887. <https://doi.org/10.1016/j.jasrep.2019.101887>
- Rodrigues, A. L., Marques, R., Dias, M. I., Prudêncio, M. I., Cardoso, G., Russo, D., Rafel, N. and Soriano, E. (2022) “Luminescence and compositional studies for the identification of “fire-set-

- ting" features at prehistoric mine La Turquesa (Catalonia, Spain)", *Journal of Radioanalytical and Nuclear Chemistry*, 331, pp. 1397-1408. <https://doi.org/10.1007/s10967-022-08198-0>
- Rodríguez Colmenero, A. and Ferrer Sierra, S. (eds.) (2006) *Excavaciones arqueológicas en Aquis Querquennis. Actuaciones en el campamento romano (1975-2005)*. Lugo: Unión Fenosa/Grupo Arqueológico Larouco/Universidade de Santiago de Compostela/Fundación Aquae Querquennae-Vía Nova.
- Salido Domínguez, J. (2020) "Un modelo de implantación de Roma en el Noroeste peninsular: la construcción de graneros sobreelevados en los castros", *Anejos. Cuadernos de Prehistoria y Arqueología de la UAM*, 4, pp. 259-271. <https://doi.org/10.15366/ane4.ochoa2020.020>
- Seabra, L., Santos, F., Vaz, F. C., Leite, J. and Tereso, J. P. (2020) "Crops behind closed walls: fortified storage at Castelinho in the Late Iron Age of NW Iberia", *Journal of Archaeological Science: Reports*, 30, 102200. <https://doi.org/10.1016/j.jasrep.2020.102200>
- Seabra, L., Carvalho, J., Ramos, R., Martín-Seijo, M., Almeida, R. and Tereso, J.P. (2023) "Arqueobotânica com vista para o Douro: frutos e sementes do sítio do Rei Ramiro (Vila Nova de Gaia, Norte de Portugal)", in Fernandes, I., Santos, M. and Correia, M. (eds.) *Amanhar a terra. Arqueologia da agricultura [Do Neolítico ao Período Medieval]*. Palmela: Município de Palmela, pp. 267-282.
- Schultz, L. G. (1964) *Quantitative interpretation of mineralogical composition X-ray and chemical data for the Pierre Shale*. US Geological Survey Professional Paper, 391.
- Schweingruber, F. H. (1990) *Anatomy of European Woods: An Atlas for the Identification of European Trees, Shrubs and Dwarf Shrubs*. Bern: Paul Haupt.
- Teira Brión, A. (2019) Cambio e resiliencia na agricultura e xestión de recursos vexetais no NW da Península Ibérica (1000 a.n.e.–400 d.n.e.). PhD thesis. Universidade de Santiago de Compostela. (Available at <http://hdl.handle.net/10347/20497>, accessed on November 2023).
- Tereso, J.P., Ramil-Rego, P. and Almeida-da-Silva, R. (2013) "Roman agriculture in the *conventus Bracaraugustanus* (NW Iberia)", *Journal of Archaeological Science*, 40, pp. 2848-2858. <http://dx.doi.org/10.1016/j.jas.2013.01.006>
- Tereso, J. P., Vaz, F.C., Silva, S. A. and Silva, A. (2023) "Consumo de plantas cultivadas e silvestres em Salreu (Estarreja, Aveiro) durante a Idade do Ferro", in Fernandes, I., Santos, M. and Correia, M. (eds.) *Amanhar a terra. Arqueologia da agricultura [Do Neolítico ao Período Medieval]*. Palmela: Município de Palmela, pp- 213-224.
- Théry-Parisot, I. and Henry, A. (2012) "Seasoned or green? Radial cracks analysis as a method for identifying the use of green wood as fuel in archaeological charcoal", *Journal of Archaeological Science*, 39, pp. 381-388. <https://doi.org/10.1016/j.jas.2011.09.024>
- Trindade, M. J., Dias, M. I., Coroado, J. and Rocha, F. (2010) "Firing Tests on Clay-Rich Raw Materials from the Algarve Basin (Southern Portugal): Study of Mineral Transformations with Temperature", *Clays and Clay Minerals*, 58, pp. 188-204. <https://doi.org/10.1346/CCMN.2010.0580205>
- Vaz, F. C., Tereso, J. P., Lemos, P. and Abranches, P. (2016) "Estudo arqueobotânico do Castro de Cidadelhe (Mesão Frio): resultados preliminares", *Estudos do Quaternário*, 15, pp. 59-69. <https://doi.org/10.30893/eq.v0i15.133>
- Vázquez Mato, M. X. (2021) "O Castro de Saceda (Cualedro). Historiografía, caracterización e cronoloxía", *Raigame*, 45, pp. 92-101.
- Verhoeven, G. (2011) "Taking computer vision aloft – archaeological three-dimensional reconstructions from aerial photographs with photoscan", *Archaeological Prospection*, 18, pp. 67-73. <https://doi.org/10.1002/arp.399>
- Vernet, J.L., Ogereau, P., Figueiral, I., Machado Yanes, C. and Uzquiano, P. (2001) *Guide d'identification des charbons de bois préhistoriques et récents. Sud-ouest de l'Europe: France, Péninsule ibérique et Îles Canaries*. Paris: CNRS Editions.
- Villar, L. (1990) "Polygonum L.", in Castroviejo, S., Laínz, M., López González, G., Montserrat, P., Muñoz Garmendia, F., Paiva, J. and Villar, L. (eds.) *Flora iberica. Plantas vasculares de la Península Ibérica e Islas Baleares. Vol II Platanaceae-Plumbaginaceae (partim)*. Madrid: Real Jardín Botánico/CSIC, 571-586.
- Zakšek, K., Oštir, K. and Kokalj, Ž. (2011) "Sky-View Factor as a Relief Visualization Technique", *Remote Sensing*, 3 (2), pp. 398-415. <https://doi.org/10.3390/rs3020398>